Magnetic Behavior of Pure Endohedral Metallofullerene Ho@C_{82}: A Comparison with Gd@C_{82}

H. J. Huang and S. H. Yang*

Department of Chemistry, The Hong Kong University of Science and Technology, Clear Water Bay, Kowloon, Hong Kong

X. X. Zhang

Department of Physics, The Hong Kong University of Science and Technology, Clear Water Bay, Kowloon, Hong Kong

Received: January 4, 1999; In Final Form: May 4, 1999

Magnetic properties of Ho@C_{82} and Gd@C_{82} were characterized in the temperature range of 1.8−100 K with an applied magnetic field up to 5 T. The isothermal magnetization curves of Gd@C_{82} and Ho@C_{82} follow the Brillouin function down to 8 and 12 K, respectively. Unlike Gd@C_{82}, the fitting to the Curie−Wiess law for Ho@C_{82} results in an effective magnetic moment which is significantly smaller than that of a free Ho^{3+} ion. The magnetic moment reduction and the imperfect paramagnetic behavior of Ho@C_{82} are ascribed to the carbon cage crystal field effect, the partial hybridization of the orbitals of the entrapped Ho atom and the carbon cage, and the interactions between the metal centers.

Introduction

Endohedral metallofullerenes have been a subject of much scientific as well as technological interest for the past few years.[1,2] On the scientific side, the formation mechanism, framework stability,[3,4] electronic structure,[4] and dynamic behavior[5,6] of metallofullerenes have attracted special attention. Practically, this type of novel materials promises a variety of important applications as superconductors, organic ferromagnets, laser media, ferroelectrics, etc.[1,2]

An intriguing aspect about metallofullerenes is the ground electronic states of the metal ions inside the carbon cage. Most monometallofullerenes M@C_{82} were shown to assume approximately an electronic structure $M^{3+}@C_{82}^{3-}$ by both experiments and calculations.[7−17] However, the divalent state was also predicted for some lanthanide metals by Nagase et al.[4,17,18] A recent XPS study showed that the electron transfer from La to the carbon cage is incomplete in La@C_{82},[19] leaving $^1/_3$ electron localized on the La ion. Pichler et al. demonstrated clearly that the Tm atom in Tm@C_{82} is divalent rather than trivalent.[20] Reports on magnetic properties of metallofullerenes also started to appear.[21−24] For example, the average magnetic measurement of La@C_{82} has been measured to be 0.38 μ_B by Funasaka et al.[22] This value is apparently larger than the magnetic moment of the free La^{3+} ion and, therefore, was attributed to an incomplete electron transfer, as observed by Kessler et al.[19]

Previous studies on the electronic structure and magnetic properties of metallofullerenes were primarily concentrated on those lanthanide elements with their 4f shells half-filled (Gd),[23] nearly full (Tm),[20] and empty or nearly empty (La).[19,22] In these cases, the orbital contribution to the total magnetic moment of the ion is small or negligible owing to the small or zero orbital angular momentum L of the magnetic orbitals. Consequently, the electron configuration, orbital hybridization, and energy level scheme of these lanthanide ions inside the carbon cage are anticipated to be much simpler than those of their homologues with a large L, e.g., Ho, Nd, and Dy. In this contribution, we present an account of our comparative studies on the magnetic properties of Ho@C_{82} ($L = 6$) and Gd@C_{82} ($L = 0$). The primary goal of this work is to identify the effect of orbital angular momentum of the lanthanide ions on the magnetic properties of metallofullerenes. It should be mentioned that this metallofullerene has been isolated before and subjected to ESR studies.[25,26] In the present study, we found the Weiss temperature of Ho@C_{82} to be $\Theta = -5.41$ K, along with a dramatic reduction of the effective magnetic moment (40%) in comparison to that of the free Ho^{3+}. This is in marked contrast to Gd@C_{82}, which is shown to be perfectly paramagnetic with a magnetic moment close to that of the free Gd^{3+}. We attribute the dramatic magnetic moment reduction of Ho@C_{82} from that of the free Ho^{3+} to the carbon cage crystal field splitting of the metal orbital angular momentum states, the partial hybridization of the electron orbitals of the metal ion and the carbon cage, and the interactions between the metal centers.

Experimental Section

Carbon soot containing metallofullerenes was produced by the standard arc vaporization method using a composite anode, which contained graphite powder and lanthanide metal oxides in an atomic ratio metal/C ≈ 0.02. These two components were uniformly mixed with graphite cement (GC grade, Dylon Inc.). The mixture was pressed into the center of a 6 mm diameter graphite rod (inner diameter 4.5 mm, 12 cm long). These rods were then baked under vacuum at 1100 °C for 3 h. Afterward, the rod was subjected to a dc discharge under an He atmosphere of 125 Torr. The raw soot was collected and extracted for 24 h using DMF as the solvent.[27] The extract was filtered using a slow-rate filter paper, and a brownish green solution was obtained. After removal of DMF by vacuum evaporation, a black

* Corresponding author. E-mail: chsyang@ust.hk.

10.1021/jp990036h CCC: $18.00
Published on Web 07/22/1999

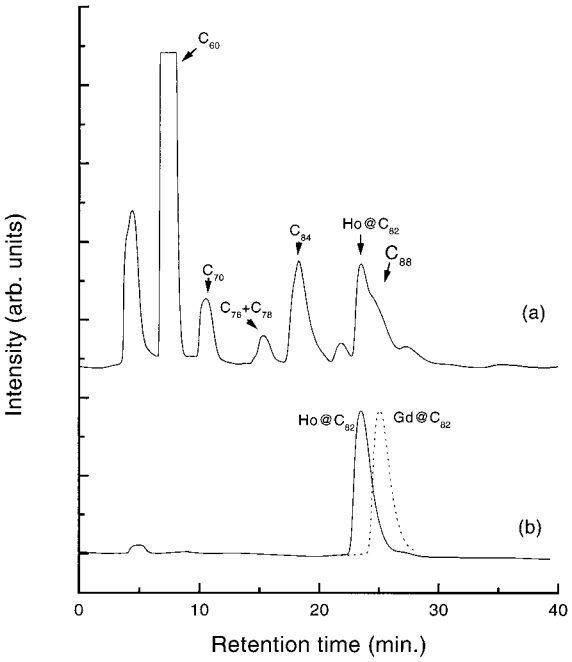

Figure 1. HPLC chromatograms of a crude metallofullerene extract redissolved in toluene (a) and a purified Ho@C_{82} sample (b).

powder was collected and redissolved in toluene. The solution was filtered with 0.2 μM disk filter (Rubbermaid Inc.) before HPLC separation. For HPLC separation, a PYE Cosmosil column (10 mm × 250 mm, Nacalai Tesque Inc.) was employed with toluene being the mobile phase. The injection volume was 5 mL, and the elution rate was 4.0 mL/min. DCI negative ion mass spectrometry (Finnigan TSQ 7000) was used to characterize the composition of the samples. The weight of our sample was obtained by weighing the dried metallofullerene powder in a precision balance (Autobalance Model AD-6). XPS measurements were carried out using monochromatized Al Kα radiation ($h\nu$ = 1486.6 eV) with an instrumental energy resolution of ~0.5 eV (Perkin-Elmer PHI 5600).

The metallofullerenes were purified immediately before the magnetic measurements to avoid oxidation. Special caution was taken in handing the metallofullerene samples. For example, the sample transfer was normally carried out under a nitrogen atmosphere. However, our experience shows that the exposure of the metallofullerenes to air for a few days did not cause significant oxidation of the species. The magnetic characterization of the pure metallofullerenes was carried out on a Quantum-Design SQUID magnetometer equipped with 5 T magnet in the temperature range between 1.8 and 300 K. The sample for the magnetic characterization was in powder form and weighed 0.9 mg for Ho@C_{82} and 2.5 mg for Gd@C_{82}. The powder samples were wrapped in a very small and thin Teflon tape for the magnetic measurements. A blank experiment on the Teflon tape was carried out, and its magnetic response was found to be negligible.

Results and Discussion

Figure 1a shows an HPLC trace of the crude extract redissolved in toluene after evaporation of DMF. A prominent peak appears at ~23.5 min, which is absent for samples produced from arc-discharge of a pure carbon electron. This peak is apparently from Ho@C_{82}, as identified by the mass spectrum shown in Figure 2. Because the peak of Ho@C_{82} is somewhat overlapped with that of C_{88} right after it, we collected only the eluate fraction before the C_{88} shoulder. Figure 1b shows

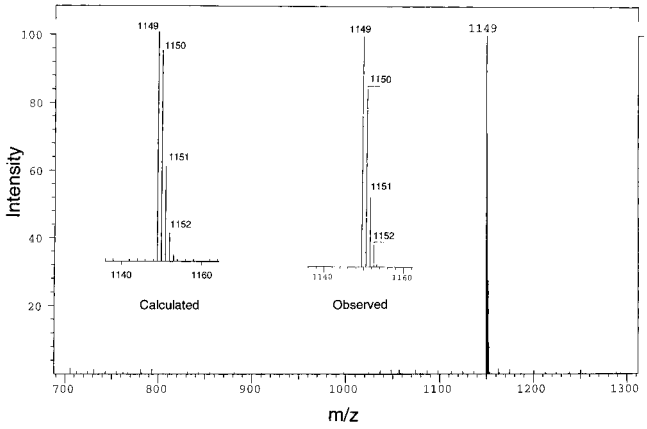

Figure 2. DCI methane negative ion mass spectrum of a purified Ho@C_{82} sample. The inset shows the observed and calculated isotope distributions of Ho@C_{82}.

the HPLC profile of the collected fraction, which exhibits a single clean peak. In the same figure, an HPLC trace of purified Gd@C_{82} under identical elution conditions is presented, and a longer retention time is revealed for Gd@C_{82} than for Ho@C_{82}. The mass spectrum shown in Figure 2 was obtained for the purified Ho@C_{82} sample. As shown in Figure 2, the observed isotope distribution is consistent with the expected isotope distribution for Ho@C_{82}. The intensities of empty fullerenes are nearly 2 orders of magnitude smaller than that of Ho@C_{82}, suggesting that the purity of our sample is ~98%.

To characterize the magnetic behavior of the endohedral metallofullerenes, the temperature-dependent magnetization in a low applied magnetic field of 50 Oe was measured in zero-field-cooled and field-cooled processes. No blocking or freezing of magnetic moments was observed down to 1.8 K for both Gd@C_{82} and Ho@C_{82}. Figure 3 shows the reciprocal of the magnetic susceptibility for the two metallofullerenes as a function of temperature measured in a magnetic field of 0.1 and 0.2 T, respectively. Careful examination in the data revealed that, in the high-temperature range (T > 40 K for Gd@C_{82} and T > 20 K for Ho@C_{82}), the magnetization follows the Cuire−Weiss law quite nicely:

$$\chi - \chi_0 = C/(T - \Theta) \qquad (1)$$

where $C = N\mu_{\text{eff}}^2/(3Ak_B) = Ng^2(J(J+1)\mu_B^2/(3Ak_B)$, Θ ($= C\gamma\rho$) is the Weiss temperature which reflects the strength of the interactions between the particles, and A is molecular weight per mole. γ is the molecular field constant.

By fitting the temperature-dependent magnetic susceptibility data in Figure 3 to eq 1, we find, for Gd@C_{82}, C = 4.85 × 10^{-3} emu·K/(g·Oe) and Θ = 0.053 K and, for Ho@C_{82}, C = 4.33 × 10^{-3} emu·K/(g·Oe) and Θ = −5.41 K. The fitted values of χ_0 are negligibly small for both metallofullerenes. From the C values, we obtain μ_{eff}(Gd@C_{82}) = 6.66 μ_B and μ_{eff}(Ho@C_{82}) = 6.30 μ_B. The effective magnetic moment of Gd@C_{82} we obtained is quite consistent with that measured by Funasaka et al.[22] It is somewhat smaller than the magnetic moment of the free Gd^{3+} ion (7.94 μ_B). This difference was not accounted for previously. One could imagine an antiparallel arrangement between the spin localized on Gd and that on the carbon cage, giving approximately S = 3. The resulting magnetic moment can be calculated to 6.93 μ_B, a value remarkably close to what was measured for Gd@C_{82}. This interaction is likely through the 5d orbitals of the lanthanide ion. The fact that Gd@C_{82} is EPR silent could be readily attributed to this coupling. An

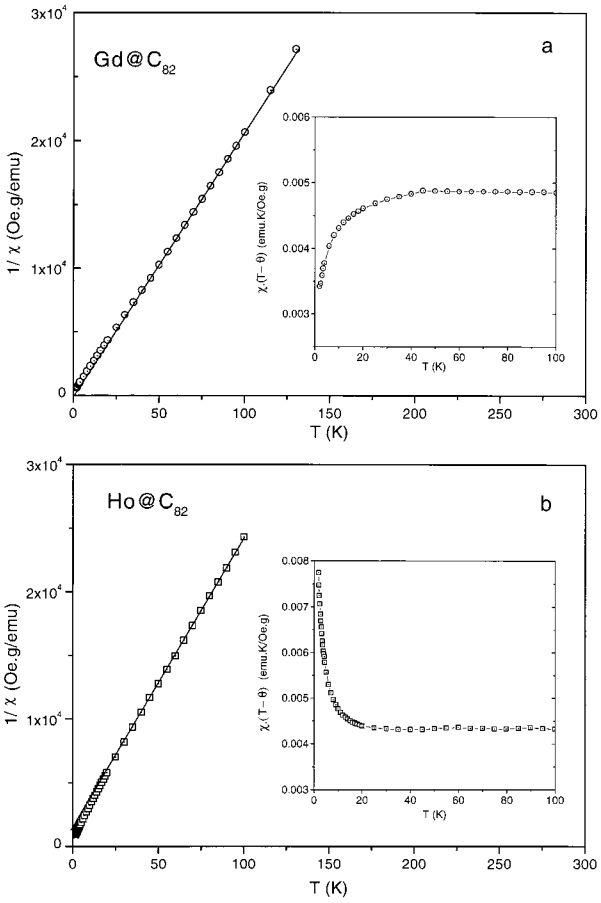

Figure 3. Reciprocal magnetic susceptibilty as a function of temperature obtained at $H = 0.1$ T for Gd@C_{82} (a) and 0.2 T for Ho@C_{82} (b). The insets show the corresponding $C = \chi(T - \Theta)$ as a function of temperature.

alternative explanation is that the negatively charged carbon cage may be substantially diamagnetic so that part of the paramagnetic response of the Gd^{3+} ion has been canceled.

On the other hand, the measured magnetic moment of Ho@C_{82} (6.30 μ_B) is much smaller than the theoretical values for both the free Ho^{3+} (10.6 μ_B) and the free Ho^{2+} (9.5 μ_B). Interestingly, the value we obtained with pure Ho@C_{82} is very close to that obtained by Diggs et al. (6.31 μ_B) using a fullerene mixture containing trace amount of Ho@C_{82}.[21] To make a more meaningful comparison, it is necessary to know the oxidation state of Ho inside the carbon cage. Figure 4 shows the XPS patterns of Ho@C_{82} and $HoCl_3 \cdot 6H_2O$ in the 3d core level region. The similarity of the two XPS patterns implies an approximately trivalent state of Ho inside the carbon cage. It is important to notice that back electron transfer from the cage to the metal 5d orbitals may be possible as pointed out by Nagase et al.[5] It appears that the magnetic moment of Ho^{3+} plunges from 10.6 to 6.3 μ_B due to the carbon caging. The more dramatic magnetic moment reduction of Ho^{3+} due to the surrounding carbon cage in comparison to that of Gd^{3+} may be explained by noticing the large orbital angular momentum of the magnetic orbitals of Ho^{3+}. The carbon cage crystal field and orbital hybridization may partially quench the orbital angular momentum, leading to the magnetic moment reduction. In addition, it is likely that the spin localized on Ho^{3+} and that localized on C_{82}^{3-} are antiferromagnetically coupled judging from the substantial negative Weiss temperature ($\Theta = -5.41$ K).

In the insets of Figure 3, $C = \chi(T - \Theta)$ is plotted as a function of temperature for both metallofullerenes. It is obvious

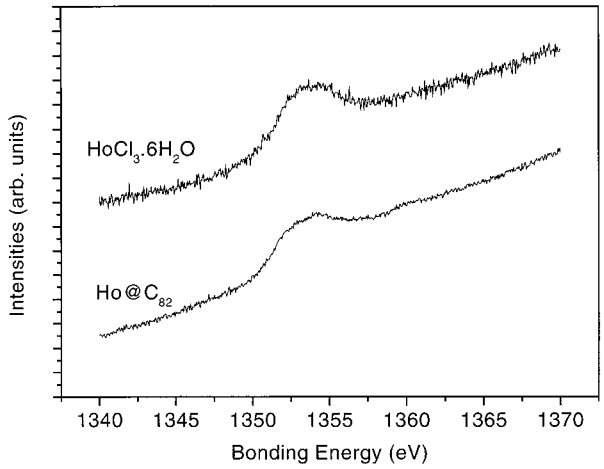

Figure 4. X-ray photoelectron spectra (XPS) of Ho@C_{82} and $HoCl_3 \cdot 3H_2O$ in the 3d core level region of Ho.

that C is independent of T above 40 K for Gd@C_{82} and above 20 K for Ho@C_{82}. For Gd@C_{82}, $\chi(T - \Theta)$ decreases below 40 K, indicating antiferromagnetic coupling between the metal centers. In contrast, $\chi(T - \Theta)$ increases for Ho@C_{82} below 20 K, suggesting ferromagnetic coupling between the metal centers. This very different magnetic behavior between Ho@C_{82} and Gd@C_{82} may also somehow related to their difference in the orbital angular momentum. The interactions between the metal centers and between the metal ion and the fullerene cage cannot be fully understood without knowing the metallofullerene assembly structures. STM studies have shown that the monometallofullerenes M@C_{82} prefer the linear, or ring-shaped, head-to-tail structures.[28−30] We have also recently observed long-chain head-to-tail structures of M@C_{82} by TEM.[31] These structures are favorable because of the sizable electric dipole moment along the symmetry axis of the metallofullerene molecules. The magnetic structure of these metallofullerenes would be one-dimensional, which involves the interaction between the encaged lanthanide ion and the carbon cage and between the metal centers. Although the distance between the lanthanide ion is quite large, such one-dimensional molecular magnetic materials have been studied for a long time, in which the distance between the lanthanide ions along the chain exceeds 1 nm.[32]

Further revelation of the peculiar magnetic behavior of Gd@C_{82} and Ho@C_{82} comes from the isothermal magnetization as a function of the applied magnetic field at different temperatures (1.8−50 K). As shown in Figure 5, *S*-like magnetization curves without a hysteresis loop were observed down to 1.8 K, exhibiting the typical paramagnetic characteristics. If the interactions between the metallofullerene particles and between the lanthanide ion and the carbon cage are negligible, the isothermal magnetization should be described by the Brillouin function

$$M = ngJ\mu_B B_J(x) \tag{2}$$

$$B_J(x) = \left(\frac{2J+1}{2J}\right)\coth\left(\frac{2J+1}{2J}\right)x - \left(\frac{1}{2J}\right)\coth\left(\frac{1}{2J}\right)x \tag{3}$$

where n is the number of magnetic ions per unit mass and $x = g\mu_B H/(k_B T)$. From the above equations, the magnetization is a unique function of the parameter x for a given ideal paramagnetic material if J and g are constant, regardless of the temperature and the applied magnetic field. In other words, if we plot the measured magnetization M as a function of H/T

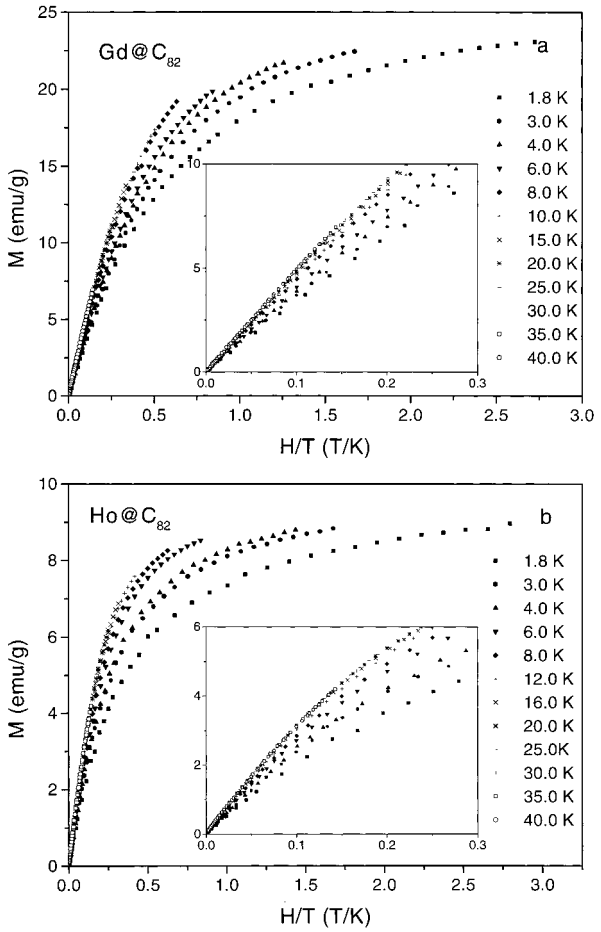

Figure 5. Isothermal magnetization as a function of H/T at different temperatures for Gd@C_{82} (a) and Ho@C_{82} (b).

using the isothermal magnetization data obtained at different temperatures, all the isothermal magnetization data points should collapse on the master curve expressed in eqs 2 and 3. Thus, by fitting the isothermal magnetization data to the Brillouin function $B_J(x)$, one would hope to get the effective magnetic moments of metallofullerenes.

The above fitting procedure appears to be applicable to Gd@C_{82} since Gd^{3+} has a zero orbital angular momentum and a spherical electron distribution. However, this turns out to work only at temperatures above ~8 K as can be seen in Figure 5a. The resulting effective magnetic moment is 6.74 μ_B. This value is comparable with that estimated above from the Curie−Weiss law. Below ~8 K, the isothermal magnetization curves deviate significantly from the master curve and the quality of the fitting to the Brillouin function becomes increasing worse as temperature decreases. The reason is that the interaction between the metallofullerene particles becomes substantial at low temperatures as shown from the magnetic susceptibility data. For Ho@C_{82}, the deviation of the isothermal magnetization data from the master curve is even more severe at low temperatures (Figure 5b). In fact, the validity of the Brillouin function may be questionable even at high temperatures since the substantial negative Weiss temperature (−5.41 K) of Ho@C_{82} already indicated an antiferromagnetic interaction between the metal and the carbon cage. The fitting of the isothermal magnetization curve above 12 K gives an effective magnetic moment of 5.43 μ_B. This value is significantly smaller than that obtained from the Curie−Weiss law.

The difference between the magnetic behavior of Gd@C_{82} and Ho@C_{82} can be more clearly appreciated by plotting the

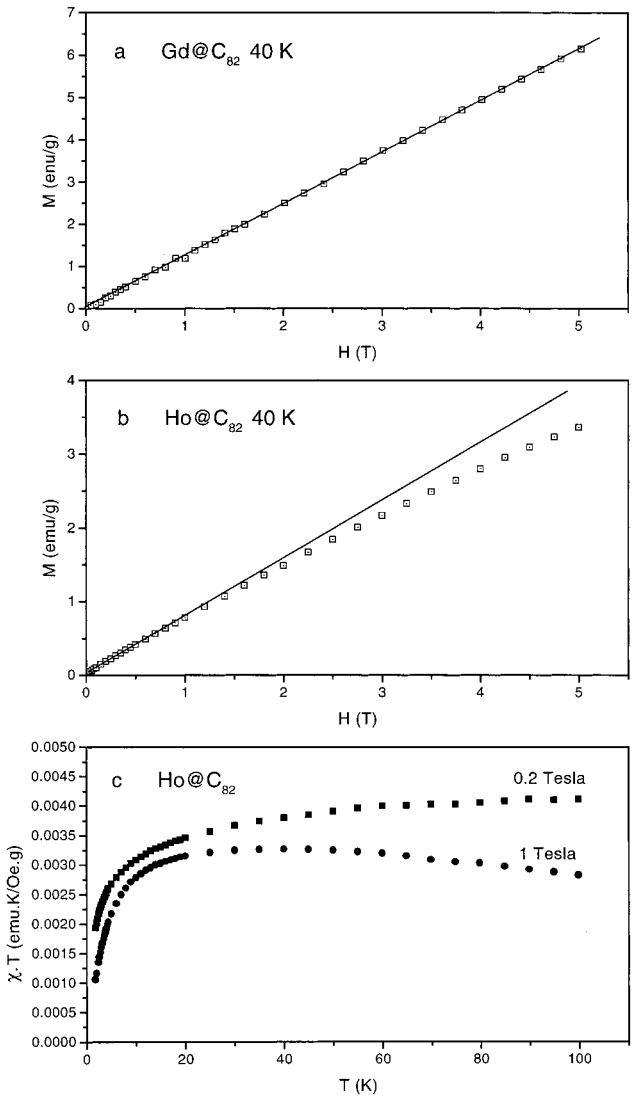

Figure 6. Magnetization as a function (M) of the applied magnetic field (H) at 50 K for Gd@C_{82} (a) and Ho@C_{82} (b). χT vs T is plotted at two different magnetic fields (c).

magnetization as a function of the applied field at a given temperature. As shown in Figure 6a, the linear relationship of M−H for Gd@C_{82} persists at the magetic field as large as 7 T. However, the M−H curve of Ho@C_{82} started to diverge from the straight line at a very low magnetic field (<1 T) (Figure 6b). This, again, may be due to the fact that the electron orbital angular momentum of Ho^{3+} is large, which induces magnetic anisotropy, whereas Gd^{3+} is relatively more isotropic owing to its spherical electron distribution. As a result of this different magnetic behavior, the determination of the effective magnetic moment of Ho@C_{82} has to be carried out in a sufficiently low magnetic field since doing so in a higher field will underestimate the effective magnetic moment (Figure 6c).

Summary and Conclusions

In conclusion, we have measured the magnetic properties of Ho@C_{82} and Gd@C_{82} in the temperature range of 1.8−100 K with an applied magnetic field up to 5 T. No hysteresis loop was found down to 1.8 K. The isothermal magnetization curves of Gd@C_{82} and Ho@C_{82} follow the Brillouin function down to 8 and 12 K, respectively. The temperature-dependent magnetic susceptibility data of Gd@C_{82} and Ho@C_{82} obey the Curie−Weiss law above 40 K (Θ = 0.053 K) and above 20 K

($\Theta = -5.41$ K), respectively. In addition, the fitting to the Curie-Wiess law for $Ho@C_{82}$ results in an effective magnetic moment which is significantly smaller than that of a free Ho^{3+} ion. The magnetic moment reduction and the imperfect paramagnetic behavior of $Ho@C_{82}$ are ascribed to the carbon cage crystal field effect, the partial hybridization of the orbitals of the entrapped Ho atom and the carbon cage, and the interactions between the metal centers.

Acknowledgment. This work was supported by the UGC of Hong Kong (Grants RGC HKUST 601/95P and RGC HKUST 6111/98P). The authors thank X. R. Wang for stimulating discussions.

References and Notes

(1) Bethune, D. S.; Johnson, R. D.; Salem, J. R.; de Vries, M. S.; Yannoni, C. S. *Nature* **1993**, 366, 123 and references therein.

(2) Shinohara, H. Endohedral Metallofullerenes: Structures and Electronic Properties. *Adv. Met. Semicond. Clusters* **1998**, *4*, 205−226.

(3) Nagase, S.; Kobayashi, K.; Akasaka, T. J. *Comput. Chem.* **1998**, *19*, 232.

(4) Kobayashi, K.; Nagase, S. *Chem. Phys. Lett.* **1998**, *282*, 325.

(5) Aksaka, T.; Nagase, S.; Kobayashi, K.; Walchli, M.; Yamamoto, K.; Funasaka, H.; Kako, M.; Hoshino, T.; Erata, T. *Angew. Chem., Int. Ed. Engl.* **1997**, *36*, 1643.

(6) Sato, W.; Sueki, K.; Kikuchi, K.; Kobayashi, K.; Suzuki, S.; Achiba, Y.; Nakahara, H.; Ohkuba, Y.; Ambe, F.; Asai, K. *Phys. Rev. Lett.* **1998**, *80*, 133.

(7) Moro, L.; Ruoff, R. S.; Becker, C. H.; Lorents, D. C.; Malhotra, R. *J. Phys. Chem.* **1993**, *97*, 6801.

(8) Wang, Y.; Tomanek, D.; Ruoff, R. S. *Chem. Phys. Lett.* **1993**, *208*, 79.

(9) Yannoni, C. S.; Hoinkis, M.; de Vries, M. S.; Bethune, D. S.; Salem, J. R.; Crowder, M. S.; Johnson, R. D. *Science* **1992**, *256*, 1191.

(10) Weaver, J. H.; Chai, Y.; Kroll, G. H.; Jin, C.; Ohno, T. R.; Haufler, R. E.; Guo, T.; Alford, J. M.; Conceicao, J.; Chibante, L. P. F.; Jain, A.; Palmer, G.; Smalley, R. E. *Chem. Phys. Lett.* **1992**, *190*, 460.

(11) Kikuchi, K.; Suzuki, S.; Nakao, Y.; Nakahara, N.; Wakabayashi, T.; Shiromaru, H.; Saito, K.; Ikemoto. I.; Achiba, Y. *Chem. Phys. Lett.* **1993**, *216*, 67.

(12) Poirier, D. M.; Knupfer. M.; Weaver, J. H.; Andreoni. W.; Laasonen, K.; Parinello, M.; Bethune, D. S.; Kikuchi, K.; Achiba, Y. *Phys. Rev. B* **1994**, *49*, 17403.

(13) Kikuchi. K.; Nakao, Y.; Suzuki, S.; Achiba, Y. *J. Am. Chem. Soc.* **1994**, *116*, 9367.

(14) Ding, J. Q.; Yang, S. H. *J. Am. Chem. Soc.* **1996**, *118*, 11254.

(15) Ding, J. Q.; Lin, N.; Weng, L.-T.; Cue, N.; Yang, S. H. *Chem. Phys. Lett.* **1996**, *261*, 92.

(16) Ding, J. Q.; Weng, L.-T.; Yang, S. H. *J. Phys. Chem.* **1996**, *100*, 11120.

(17) Nagase, S.; Kobayashi, K. *Chem. Phys. Lett.* **1993**, *214*, 57.

(18) Nagase, S.; Kobayashi, K. *Chem. Phys. Lett.* **1994**, *228*, 106.

(19) Kessler, B.; Bringer, A.; Cramm, S.; Schlebusch, C.; Eberhardt, W.; Suzuki, S.; Achiba, Y.; Esch, F.; Barnaba, M.; Cocco, D. *Phys. Rev. Lett.* **1997**, *79*, 2289.

(20) Pichler, T.; Golden, M. S.; Knupfer, M.; Fink, J.; Kirbach, U.; Kuran, P.; Dunsch, L. *Phys. Rev. Lett.* **1997**, *79*, 3026.

(21) Diggs, B.; Zhou, A.; Silva, C.; Kirkpatrick, S.; Nuhfer, N. T.; McHenry, M. E.; Petasis, D.; Majetich, S. A.; Brunett, B.; Artman, J. O.; Staley, S. W. *J. Appl. Phys.* **1994**, *75*, 5879.

(22) Funasaka, H.; Sugiyama, K.; Yamamoto, K.; Takahashi, T. *J. Phys. Chem.* **1995**, *99*, 1826 and references therein.

(23) Funasaka, H.; Sakurai, K.; Oda, Y.; Yamamoto, K.; Takahashi, T. *Chem. Phys. Lett.* **1995**, *232*, 273.

(24) Dunsch, L.; Eckert, D.; Frohner, J.; Bartl, A.; Kuran, P.; Wolf, M.; Muller, K. *Recent Advances in Fullerenes, Electrochemical Society Proceedings*; Electrochemical Society: Pennington, NJ, 1998; V98-8, pp 955−966.

(25) Bartle, A.; Dunsch, L.; Kirbach, U. *Solid State Commun.* **1995**, *94*, 827.

(26) Knapp, C.; Weiden, N.; Dinse, K.-P. *Appl. Phys. A* **1998**, *66*, 249.

(27) Ding, J. Q.; Yang, S. H. *Chem. Mater.* **1996**, *8*, 2824.

(28) Shinohara, H.; Inakuma, M.; Kishida M.; Yamazaki, S.; Hashizume, T.; Sakurai, T. *J. Phys. Chem.* **1995**, *99*, 13769.

(29) Lin, N.; Huang, H. J.; Yang, S. H.; Cue, N. *J. Phys. Chem. A* **1998**, *102*, 4411.

(30) Lin, N.; Huang, H. J.; Yang, S. H.; Cue, N. *Phys. Rev. B* **1998**, *58*, 2126.

(31) Huang, H. J.; Yang, S. H. Unpublished results.

(32) Benelli, C.; Caneschi, A.; Gatteschi, D.; Sessoli, R. *Inorg. Chem.* **1993**, *32*, 4797.